

An Optimal Control Framework for Influencing Human Driving Behavior in Mixed-Autonomy Traffic

Anirudh Chari¹, Rui Chen², Jaskaran Grover³, Changliu Liu²

Abstract—As autonomous vehicles (AVs) become increasingly prevalent, their interaction with human drivers presents a critical challenge. Current AVs lack social awareness, causing behavior that is often awkward or unsafe. To combat this, social AVs, which are proactive rather than reactive in their behavior, have been explored in recent years. With knowledge of robot-human interaction dynamics, a social AV can influence a human driver to exhibit desired behaviors by strategically altering its own behaviors. In this paper, we present a novel framework for achieving human influence. The foundation of our framework lies in an innovative use of control barrier functions to formulate the desired objectives of influence as constraints in an optimal control problem. The computed controls gradually push the system state toward satisfaction of the objectives, e.g. slowing the human down to some desired speed. We demonstrate the proposed framework’s feasibility in a variety of scenarios related to car-following and lane changes, including multi-robot and multi-human configurations. In two case studies, we validate the framework’s effectiveness when applied to the problems of traffic flow optimization and aggressive behavior mitigation. Given these results, the main contribution of our framework is its versatility in a wide spectrum of influence objectives and mixed-autonomy configurations.

I. INTRODUCTION

Autonomous vehicles (AVs) are increasingly popular on today’s roadways, largely as a result of great strides in perception, planning, and control algorithms in recent years [1]. However, these systems remain far from perfect, particularly because current AVs struggle to deal with human drivers. Many existing works treat human drivers as dynamic obstacles rather than decision-making agents [2], and this assumption often yields awkward or unsafe behavior. Addressing this problem is crucial, as AVs and human drivers will likely share the roads for many years to come [3].

Recently, the idea of a *social* AV has emerged as a potential solution to this problem, with human-AV social interactions being studied extensively [4]. The social AV is proactive rather than reactive: it leverages models of human behavior to inform its own decision-making. In particular, a social AV might strategically alter its own behavior so as to *influence* a human driver to exhibit some desired behavior. To accomplish this, the AV must exploit models not only of the human’s driving behavior but also of the change

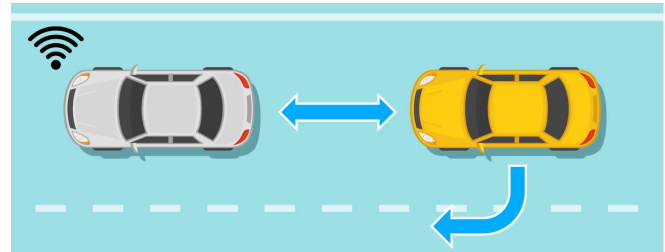


Fig. 1: A robot car is being tailgated by a human-driven car. How can the robot influence the human to increase following distance or to change lanes?

in the human’s behavior with respect to its own behavior. The concept of social influence has numerous applications in mixed-autonomy settings. In congested traffic, AVs can orchestrate cooperative merging and lane-changing maneuvers, alleviating traffic bottlenecks. In emergency situations, AVs can guide human drivers to take evasive actions that mitigate collision risks. Human influence for general human-robot collaboration is studied in [5], and applications to traffic flow optimization have been widely explored [6], [7]. Furthermore, a single-agent control framework is provided in [8], and [9], [10] provide frameworks for single-agent influence with simultaneous probing, i.e. learning human driving parameters by observing behavior.

More generally, the concept of a socially *aware* AV has been studied extensively. Awareness is a prerequisite for influence: a social AV must first understand human interactions before attempting to alter human behavior. While human influence is a very active procedure, awareness is more passive. The socially aware AV is cognizant of its effects on human behaviors and it may consider these effects during planning, but it does not necessarily seek to apply this knowledge to altering these behaviors. Social awareness functions as a significant first step toward full human-AV social interaction in mixed-autonomy settings, especially given the extensive work done in learning human driving behavior [11], [12]. Some studies have achieved superior AV control by considering human car-following [13] and lane-changing [14] behaviors. These ideas have also been employed in designing AV control frameworks [15].

Control barrier functions (CBFs) are a popular tool for safe AV control. In particular, CBFs have been employed in problems of cooperative AV merging [16], [17] and lane-changing [18]. For a thorough overview of CBFs and their applications, see [19]. In comparison to existing methods of human influence that traditionally use game-theoretic formulations [20], [21], a CBF-based approach offers guarantees

¹A. Chari is with the Illinois Mathematics and Science Academy in Aurora, IL, USA. (achari@imsa.edu)

²R. Chen and C. Liu are with the Robotics Institute at Carnegie Mellon University in Pittsburgh, PA, USA. ({ruic3, cliu6}@andrew.cmu.edu)

³J. Grover is with Amazon Robotics in North Reading, MA, USA. (jessygro@amazon.com)

This work is partially supported by the National Science Foundation, Grant No. 2144489.

of safety and convergence, resulting in more robust and predictable policies.

To the best of the authors' knowledge, the current literature on human influence is restricted either to localized objectives (e.g. following, merging) or to single-agent configurations. In this work, we aim to fill this gap. **Our main contributions are: (a) an optimal control framework for influencing human driving behavior using CBFs, with applicability to (b) various objectives of influence and (c) multi-robot and multi-human scenarios.** Section II formulates the problem of human influence. Section III presents our framework. Section IV discusses the results of principal experiments using our framework. Section V discusses the results of two case studies involving our framework. Finally, Section VI concludes our study and presents future directions.

II. PROBLEM FORMULATION

We are given a group of m human-driven cars, n robot cars, and q non-interactive background cars that travel along a multi-lane highway with L lanes. While human-driven cars react to the behavior of robot cars, background cars do not. Our objective is to compute robot car controls \mathbf{u} at each timestep that influence the human-driven cars to exhibit some desired behaviors and minimize some cost function $J(\mathbf{u})$.

In a state space \mathcal{X} , let $\mathbf{p}_H \in \mathbb{R}^m$ denote the human-driven car positions relative to some fixed starting point along their respective lanes, $\mathbf{v}_H \in \mathbb{R}^m$ their velocities in their lanes, and $\mathbf{a}_H \in \mathbb{R}^m$ their accelerations in their lanes. Similarly, let $\mathbf{p}_R \in \mathbb{R}^n$ denote positions of the robot cars along their lanes, $\mathbf{v}_R \in \mathbb{R}^n$ their velocities, and $\mathbf{a}_R \in \mathbb{R}^n$ their accelerations, and let $\mathbf{p}_B \in \mathbb{R}^q$ denote positions of the background cars along their lanes, $\mathbf{v}_B \in \mathbb{R}^q$ their velocities, and $\mathbf{a}_B \in \mathbb{R}^q$ their accelerations. Let p_{Hi} denote the position of the i -th human-driven car H_i , p_{Rj} the position of the j -th robot car R_j , and p_{Bk} the position of the k -th background car B_k . Let $l_{Hi} \in \{1, \dots, L\}$ denote the current lane of human-driven car H_i , and represent the current lanes of all human-driven cars as $\mathbf{l}_H := (l_{H1}, \dots, l_{Hm})$. Define \mathbf{l}_R for the current lanes of the robot cars and \mathbf{l}_B for the current lanes of the background cars in a similar fashion. We will assume that robot cars and background cars maintain their lanes.

Let us assume that human-driven cars follow double integrator dynamics that can be represented as

$$\dot{\mathbf{p}}_H = \mathbf{v}_H, \quad \dot{\mathbf{v}}_H = \mathbf{a}_H = \mathbf{f}(\mathbf{x}) \quad (1)$$

where \mathbf{x} is the system state and each $f_i(\mathbf{x})$ has some known parameters θ_i that define human driver i 's behavior [22]. Let us assume that the robot cars are acceleration-controlled. Their dynamics can be posed as

$$\dot{\mathbf{p}}_R = \mathbf{v}_R, \quad \dot{\mathbf{v}}_R = \mathbf{a}_R \equiv \mathbf{u}. \quad (2)$$

Let us assume that the background cars travel with constant velocities. This is a reasonable assumption because, in the absence of external influence, cars generally maintain their speed in highway settings. Then we have

$$\dot{\mathbf{p}}_B = \mathbf{v}_B, \quad \dot{\mathbf{v}}_B = \mathbf{a}_B = \mathbf{0}. \quad (3)$$

The human-driven cars have lane-change controls $\mathbf{d}_H \in \{-1, 0, 1\}^m$. Lane changing is a discrete event; lanes are updated at each timestep as

$$\mathbf{l}_H(t + \Delta t) = \mathbf{l}_H(t) + \mathbf{d}_H. \quad (4)$$

This definition encodes the actions {left, stay, right}. For human-driven car H_i we have

$$d_{Hi} = \pm(z_i^S(\mathbf{x}) \geq 0 \wedge z_i^I(\mathbf{x}) \geq 0) \quad (5)$$

where $z_i^S(\mathbf{x})$ is a lane-change safety function, $z_i^I(\mathbf{x})$ is a lane-change incentive function, and both depend again on parameters θ_i . For example, $z_i^S(\mathbf{x})$ could be a function of the space available between cars in the adjacent lane, and $z_i^I(\mathbf{x})$ could be a function of the difference in velocity or acceleration between the human's current lane and the adjacent lane. The \pm symbol exists here to denote that a lane change may occur in either direction.

We denote the human-driven cars' collective state as $\mathbf{x}_H := (\mathbf{p}_H, \mathbf{v}_H, \mathbf{l}_H)$. We denote the robot cars' collective state as $\mathbf{x}_R := (\mathbf{p}_R, \mathbf{v}_R, \mathbf{l}_R)$. We denote the background cars' collective state as $\mathbf{x}_B := (\mathbf{p}_B, \mathbf{v}_B, \mathbf{l}_B)$. The total state of our system is denoted as $\mathbf{x} := (\mathbf{x}_H, \mathbf{x}_R, \mathbf{x}_B)$.

We can formulate an arbitrary objective of influence as a constraint function $\psi : \mathcal{X} \rightarrow \mathbb{R}$ such that $\psi \geq 0$ implies that the objective is satisfied. For example, we can express influencing an upper bound v_{max} on human-driven car H_i 's velocity as $\psi = v_{max} - v_{Hi}$. Because lane changes are discrete events, we will utilize (5) to derive constraints that influence lane changes, rather than formulating constraints directly in terms of \mathbf{d}_H . For example, if z_i^I is a function of H_i 's velocity, then our constraint will be directly on H_i 's velocity. For N simultaneous influence objectives, we can derive constraints $\psi := (\psi_1, \dots, \psi_N)$. Then given some cost function $J(\mathbf{u})$, we can pose the following problem to solve for optimal robot controls \mathbf{u}^* that achieve human influence:

$$\mathbf{u}^* = \underset{\mathbf{u}}{\operatorname{argmin}} J(\mathbf{u}) \quad \text{s.t.} \quad \psi \geq \mathbf{0} \quad (6)$$

In the next section, we further derive a control constraint that yields satisfaction of the state constraint $\psi \geq \mathbf{0}$.

III. OPTIMAL CONTROL FRAMEWORK

In this section, we present the optimal control framework in detail. We first describe the intuition motivating the framework's design. We then review and define some key properties of time derivatives. Next, we outline the procedure by which constraints on the robot controls are derived. Finally, we pose the general optimal control problem for achieving human influence.

A. Preliminary: Control Barrier Functions

In [23], CBFs are employed to compute controls for a group of *dog robots* that herd a flock of *sheep agents*. The sheep aim to reach some goal location, and the dogs must prevent the sheep from breaching some spatial protected zone. Crucially, the dog robots exploit knowledge of the dog-sheep interaction dynamics to achieve this objective.

Similarly, here we have a group of human-driven cars that exhibit some defined behavior, and a group of surrounding robot cars must influence this behavior with the objective of enforcing some abstract “protected zone.”

We claim that CBFs are a useful tool for enforcing this protected zone. Using CBFs, we define our protected zone as a barrier function $h : \mathcal{X} \rightarrow \mathbb{R}$ where $h \geq 0$ implies safety in our system, meaning satisfaction of our influence objective. To push our system toward safety over time, we can enforce $\dot{h} + p_1 h \geq 0$, where p_1 is a design parameter and $p_1 > 0$. To derive an explicit constraint on robot controls, we might compute further time derivatives of h and express our constraint in terms of \ddot{h} or \dddot{h} . In general, an N -th order constraint is given as $(1 + p_1 s)(1 + p_2 s) \cdots (1 + p_N s)h \geq 0$ where s is the differentiation operator. We expand this to $h + \sum_{i=0}^N \alpha_i h^{(i)} \geq 0$ where $h^{(i)}$ denotes the i -th time derivative of h . It remains that our system tends toward $h \geq 0$, and thus the protected zone is enforced.

B. Preliminary: Time Derivative Properties

In general, we can make use of the following discrete approximations for computing time derivatives:

$$\dot{f}_i = \frac{df_i}{dt} \approx \frac{f_i - a_{Hi}}{\Delta t} \quad (7)$$

$$\dot{u}_j = \frac{du_j}{dt} \approx \frac{u_j - a_{Rj}}{\Delta t} \quad (8)$$

where Δt is the discretization timestep.

Definition 1 (Direct influence). We refer to a human-driven car H_i as *directly influenced* by a robot car R_j if $f_i(\mathbf{x})$ is dependent on \mathbf{x}_{Rj} , i.e. $\nabla_{\mathbf{x}_{Rj}} f_i(\mathbf{x}) \neq \mathbf{0}$.

Consider a human-driven car H_i that is directly influenced by a robot car R_j . Then when computing the time derivative of f_i , we have

$$\begin{aligned} \dot{f}_i(\mathbf{x}) &= \nabla f_i(\mathbf{x}(t))^T \dot{\mathbf{x}}(t) \\ &= \frac{\partial f_i}{\partial p_{Hi}} \dot{p}_{Hi} + \frac{\partial f_i}{\partial v_{Hi}} \dot{v}_{Hi} + \frac{\partial f_i}{\partial p_{Rj}} \dot{p}_{Rj} + \frac{\partial f_i}{\partial v_{Rj}} \dot{v}_{Rj} \\ &= \frac{\partial f_i}{\partial p_{Hi}} v_{Hi} + \frac{\partial f_i}{\partial v_{Hi}} a_{Hi} + \frac{\partial f_i}{\partial p_{Rj}} v_{Rj} + \frac{\partial f_i}{\partial v_{Rj}} u_j \\ &= \lambda_{ij} + \frac{\partial f_i}{\partial v_{Rj}} u_j \end{aligned} \quad (9)$$

where $\lambda_{ij} := \frac{\partial f_i}{\partial p_{Hi}} v_{Hi} + \frac{\partial f_i}{\partial v_{Hi}} a_{Hi} + \frac{\partial f_i}{\partial p_{Rj}} v_{Rj}$. Notice that this gives us an explicit relationship between human actions and robot controls.

C. Constraint Derivation

Let $y^{(c)}$ denote the c -th time derivative of y . For our overall state constraint $\psi \geq \mathbf{0}$, recall that each individual c -th order constraint is defined as $\psi_i(\mathbf{p}_H^{(c)}, \mathbf{p}_R^{(c)}, \mathbf{p}_B^{(c)})$ and encodes some desired high-level objective such that $\psi_i \geq 0$ iff the objective is satisfied. Thus, ψ_i can be treated as a barrier function h , as outlined in Section III-A.

Note that not all terms in ψ_i are necessarily nonzero, e.g. an objective may only involve a subset of the cars in \mathbf{x} . Also

note that we require the same relative degree for all terms, although this is sometimes aided by approximating higher-order terms using lower-order terms.

We compute b time derivatives of ψ_i to obtain

$$\begin{aligned} \psi_i^{(b)}(\mathbf{p}_H^{(b+c)}, \mathbf{p}_R^{(b+c)}) &:= \psi_i^h(\dot{\mathbf{f}}, \dot{\mathbf{u}}) \\ &\equiv \psi_i^h(\dot{\mathbf{f}}_{-\varphi}, \dot{\mathbf{f}}_{\varphi}, \dot{\mathbf{u}}) \end{aligned} \quad (10)$$

where $\dot{\mathbf{f}}_{\varphi}$ is the set of all \dot{f}_i such that human-driven car H_i is directly influenced by some robot car R_j , and $\dot{\mathbf{f}}_{-\varphi}$ is the set of all \dot{f}_i such that human-driven car H_i is not directly influenced by any robot car R_j . Notice that we no longer have a \mathbf{p}_B term, since we assume constant velocities for background cars.

We first leverage (9) to convert $\dot{\mathbf{f}}_{\varphi}$ terms to \mathbf{u} terms, yielding the equivalent form $\psi_i^{(b)}(\dot{\mathbf{f}}_{-\varphi}, \mathbf{u}, \dot{\mathbf{u}})$. Then, we leverage (7) to convert $\dot{\mathbf{f}}_{-\varphi}$ terms to \mathbf{f} terms, and (8) to convert $\dot{\mathbf{u}}$ terms to \mathbf{u} terms, yielding a more usable function $\psi_i^h(\mathbf{f}, \mathbf{u})$. Finally, we can express our initial objective as the following CBF constraint:

$$g_i(\mathbf{x}, \mathbf{f}, \mathbf{u}) := \psi_i^h + \sum_{j=0}^{b-1} \alpha_j \psi_i^{(j)} \geq 0 \quad (11)$$

Using CBFs, we have now effectively translated our original state constraint $\psi_i \geq 0$ into a control constraint $g_i \geq 0$.

D. Optimization Problem

We use the above process to derive N linear constraints:

$$\mathbf{g}(\mathbf{x}, \mathbf{f}, \mathbf{u}) := \begin{bmatrix} g_1(\mathbf{x}, \mathbf{f}, \mathbf{u}) \\ \vdots \\ g_N(\mathbf{x}, \mathbf{f}, \mathbf{u}) \end{bmatrix} \geq \mathbf{0} \quad (12)$$

We can then adapt (6) to pose the following optimization problem to solve for controls \mathbf{u}^* that push the system toward $\psi \geq \mathbf{0}$, i.e. satisfaction of the objectives of influence:

$$\mathbf{u}^* = \underset{\mathbf{u}}{\operatorname{argmin}} J(\mathbf{u}) \quad \text{s.t.} \quad \mathbf{g}(\mathbf{x}, \mathbf{f}, \mathbf{u}) \geq \mathbf{0} \quad (13)$$

The problem (13) is feasible if (12) is feasible (i.e. the half-spaces created by g_1, \dots, g_N intersect) and (12) intersects with the control limits. In this paper, we assume that (13) is always feasible. To ensure such feasibility in practice, one must solve the synthesis problem, as introduced in [24], [25].

IV. PRINCIPAL EXPERIMENTS

In this section, we verify the feasibility of our framework under various objectives by simulating nine low-level scenarios. We also provide an example constraint derivation for one scenario to illustrate the process.

A. Human Behavior Models

Here we specify the behavior models used for human driver control. For longitudinal control (i.e., car-following), we define each $f_i(\mathbf{x})$ using the intelligent driver model (IDM) [22]. Thus, we have

$$f_i := a_i^{max} \left(1 - \left(\frac{v_{Hi}}{v_{0i}} \right)^4 - \left(\frac{s^*(v_{Hi}, \Delta v_i)}{s_i} \right)^2 \right) \quad (14)$$

with

$$s^*(v_{H_i}, \Delta v_i) := s_{0i} + v_{H_i}T + \frac{v_{H_i}\Delta v_i}{2\sqrt{a_i^{max}b_i^{max}}} \quad (15)$$

where a_i^{max} is the maximum acceleration of H_i , b_i^{max} is its maximum deceleration, v_{0i} is its desired velocity, s_{0i} is its desired following distance, s_i is its current following distance, and Δv_i is the current difference between its own velocity and the velocity of the preceding car.

For lateral control (i.e., lane-changing), we define the safety function for H_i as

$$z_i^S := p^F - p_{H_i} - s_i^{min} \geq 0 \wedge p_{H_i} - p^B - s_i^{min} \geq 0 \quad (16)$$

where p^F is the position of the car in front of H_i in the adjacent lane, p^B is the position of the car behind H_i in the adjacent lane, and s_i^{min} is some minimum distance threshold desired by H_i . We define the incentive function for H_i as

$$z_i^I := v^F - v_{H_i} - \Delta v_i^{th} \geq 0 \quad (17)$$

where v^F is the velocity of the car in front of H_i in the adjacent lane, and Δv_i^{th} is some minimum threshold desired by H_i for the velocity difference between the two cars. Together, these two criteria encode that a human driver changes lanes if there is ample space in the adjacent lane and a potential increase in velocity following the lane change. This is similar to real-world highway lane change behavior, where humans seek to increase their speed up to some desired value, as can be seen in IDM.

B. Experimental Scenarios

Here we introduce nine low-level scenarios to demonstrate the feasibility of our framework under various objectives. We examine three single-human single-robot scenarios (**S1-S3**), three single-human multi-robot scenarios (**SM1-SM3**), and three multi-human multi-robot scenarios (**M1-M3**). For all scenarios, we have $\Delta t = 0.01$ s, car length $\ell = 5$ m, and each robot car R_j has bounded velocity $v_{R_j} \in [0, 35]$ m/s and bounded acceleration $a_{R_j} \in [-4, 2]$ m/s². For human behavior, we have $v_{0i} = 35$ m/s, $s_i^{min} = 10$ m, $\Delta v_i^{th} = 3$ m/s for all H_i , and humans follow the normal driving IDM parameters given in [26]. For simplicity, we omit the lane-change incentive criterion in scenarios **M1-M3**. We use the cost function $J(\mathbf{u}) = \|\mathbf{u}\|_2^2$ to minimize control effort in our optimization. Fig. 2 details **S1-S3** and **SM1-SM3** and their simulation results, Fig. 3 details **M1-M3** and their simulation results, and Fig. 4 visualizes **M1**.

C. Example Derivation

Here we provide an example derivation of the optimal control problem for scenario **M1**. This includes the human driver lane change's forward and backward safety criteria. First, we wish to enforce a minimum distance s_2^{min} between R_1 and H_2 to allow for a lane change. We express this as

$$\psi_F := p_{R_1} - p_{H_2} - s_2^{min}. \quad (18)$$

The time derivatives of ψ_F are as follows:

$$\begin{aligned} \dot{\psi}_F &= \dot{p}_{R_1} - \dot{p}_{H_2} \\ \ddot{\psi}_F &= \ddot{p}_{R_1} - \ddot{p}_{H_2} = u_1 - f_2 \\ \dddot{\psi}_F &= \dot{u}_1 - \dot{f}_2 := \psi_F^h \end{aligned} \quad (19)$$

Notice that $\ddot{\psi}_F$ contains u_1 but not u_2 , so we take an additional time derivative of ψ_F to obtain a \dot{f}_2 term in $\dddot{\psi}_F$. This allows us to exploit the time derivative properties. We apply (9) to ψ_F^h to obtain $\dot{u}_1 - \frac{\partial f_2}{\partial v_{R_2}}u_2 - \lambda_{22}$. Intuitively, we have now translated human actions into robot controls. Now, we just need to standardize everything to \mathbf{u} terms rather than $\dot{\mathbf{u}}$, so we apply (8) to ψ_F^h to obtain

$$\frac{1}{\Delta t}u_1 - \frac{\partial f_2}{\partial v_{R_2}}u_2 - \frac{a_{R_1}}{\Delta t} - \lambda_{22}. \quad (20)$$

Finally, we have an explicit function of robot controls u_1 and u_2 , so we can express our CBF constraint as

$$g_F(\mathbf{x}, \mathbf{f}, \mathbf{u}) = \psi_F^h + \alpha_2^F \ddot{\psi}_F + \alpha_1^F \dot{\psi}_F + \alpha_0^F \psi_F \geq 0. \quad (21)$$

Next, we wish to enforce a minimum distance s_2^{min} between H_2 and H_1 to allow for a lane change. We express this as

$$\psi_B := p_{H_2} - p_{H_1} - s_2^{min}. \quad (22)$$

Notice that here, ψ_B is not a function of the robot state. The time derivatives of ψ_B are as follows:

$$\begin{aligned} \dot{\psi}_B &= \dot{p}_{H_2} - \dot{p}_{H_1} \\ \ddot{\psi}_B &= \ddot{p}_{H_2} - \ddot{p}_{H_1} = f_2 - f_1 \\ \ddot{\psi}_B &= \dot{f}_2 - \dot{f}_1 := \psi_B^h \end{aligned} \quad (23)$$

We reached $\ddot{\psi}_B$ to obtain $\dot{\mathbf{f}}$, so now we can again exploit the time derivative properties. We apply (9) to ψ_B^h to obtain

$$-\frac{\partial f_1}{\partial v_{R_1}}u_1 + \frac{\partial f_2}{\partial v_{R_2}}u_2 - \lambda_{11} + \lambda_{22}. \quad (24)$$

We now have an explicit function of u_1 and u_2 , so we can express our CBF constraint as

$$g_B(\mathbf{x}, \mathbf{f}, \mathbf{u}) = \psi_B^h + \alpha_2^B \ddot{\psi}_B + \alpha_1^B \dot{\psi}_B + \alpha_0^B \psi_B \geq 0. \quad (25)$$

We have derived the linear constraints

$$\mathbf{g}(\mathbf{x}, \mathbf{f}, \mathbf{u}) := \begin{bmatrix} g_F(\mathbf{x}, \mathbf{f}, \mathbf{u}) \\ g_B(\mathbf{x}, \mathbf{f}, \mathbf{u}) \end{bmatrix} \geq \mathbf{0}. \quad (26)$$

We can formulate this as

$$A^{M1}\mathbf{u} \geq \mathbf{b}^{M1} \quad (27)$$

where

$$A^{M1} := \begin{bmatrix} (\alpha_2^F + \frac{1}{\Delta t}) & -\frac{\partial f_2}{\partial v_{R_2}} \\ -\frac{\partial f_1}{\partial v_{R_1}} & \frac{\partial f_2}{\partial v_{R_2}} \end{bmatrix}, \quad \mathbf{b}^{M1} := \begin{bmatrix} \beta^F \\ \beta^B \end{bmatrix}$$

with $\beta^F := \frac{a_{R_1}}{\Delta t} + \lambda_{22} + \alpha_2^F f_2 - \alpha_1^F \dot{\psi}_F - \alpha_0^F \psi_F$ and $\beta^B := \lambda_{11} - \lambda_{22} - \alpha_2^B \ddot{\psi}_B - \alpha_1^B \dot{\psi}_B - \alpha_0^B \psi_B$. Finally, we can pose the following QP to solve for the robot controls at each timestep:

$$\mathbf{u}^* = \underset{\mathbf{u}}{\operatorname{argmin}} \|\mathbf{u}\|_2^2 \quad \text{s.t.} \quad A^{M1}\mathbf{u} \geq \mathbf{b}^{M1} \quad (28)$$

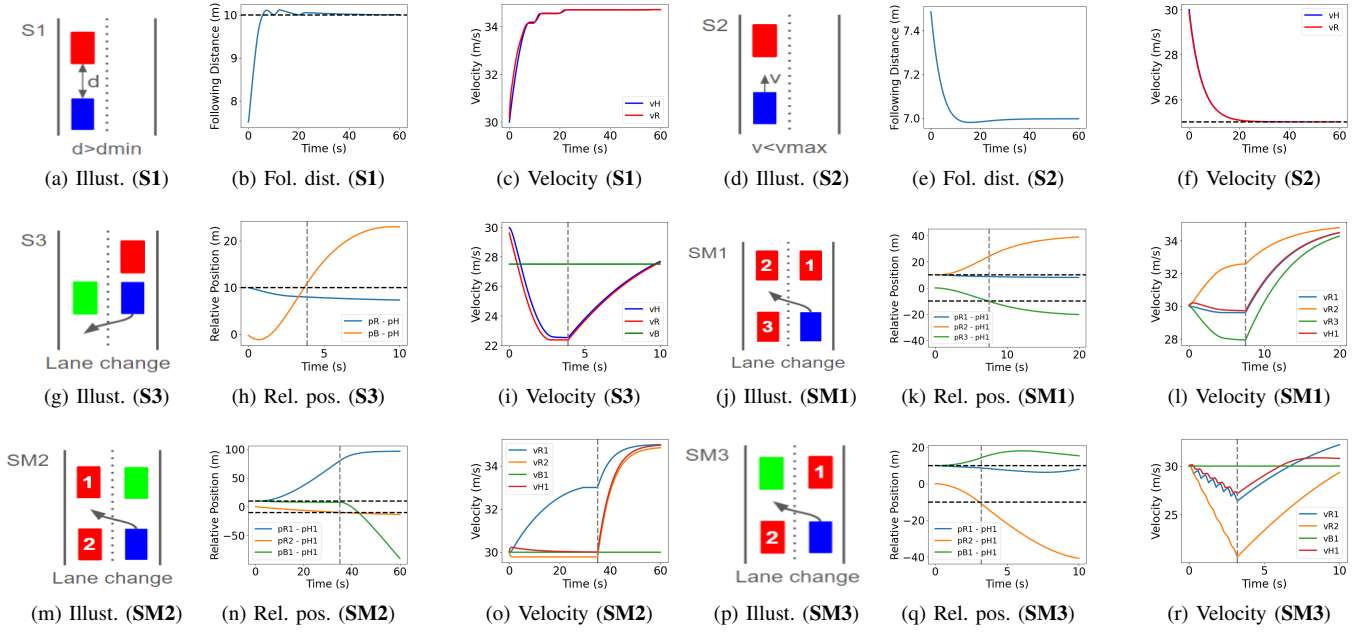


Fig. 2: Illustrations, human-relative position vs. time graphs, and velocity vs. time graphs for scenarios **S1-S3** and **SM1-SM3**. In illustrations, red boxes are robot cars, blue boxes are human-driven cars, and green boxes are background cars. In graphs, black dotted horizontal lines denote lower or upper bounds on the value via the influence objective, and gray dotted vertical lines denote the time at which a lane change occurs.

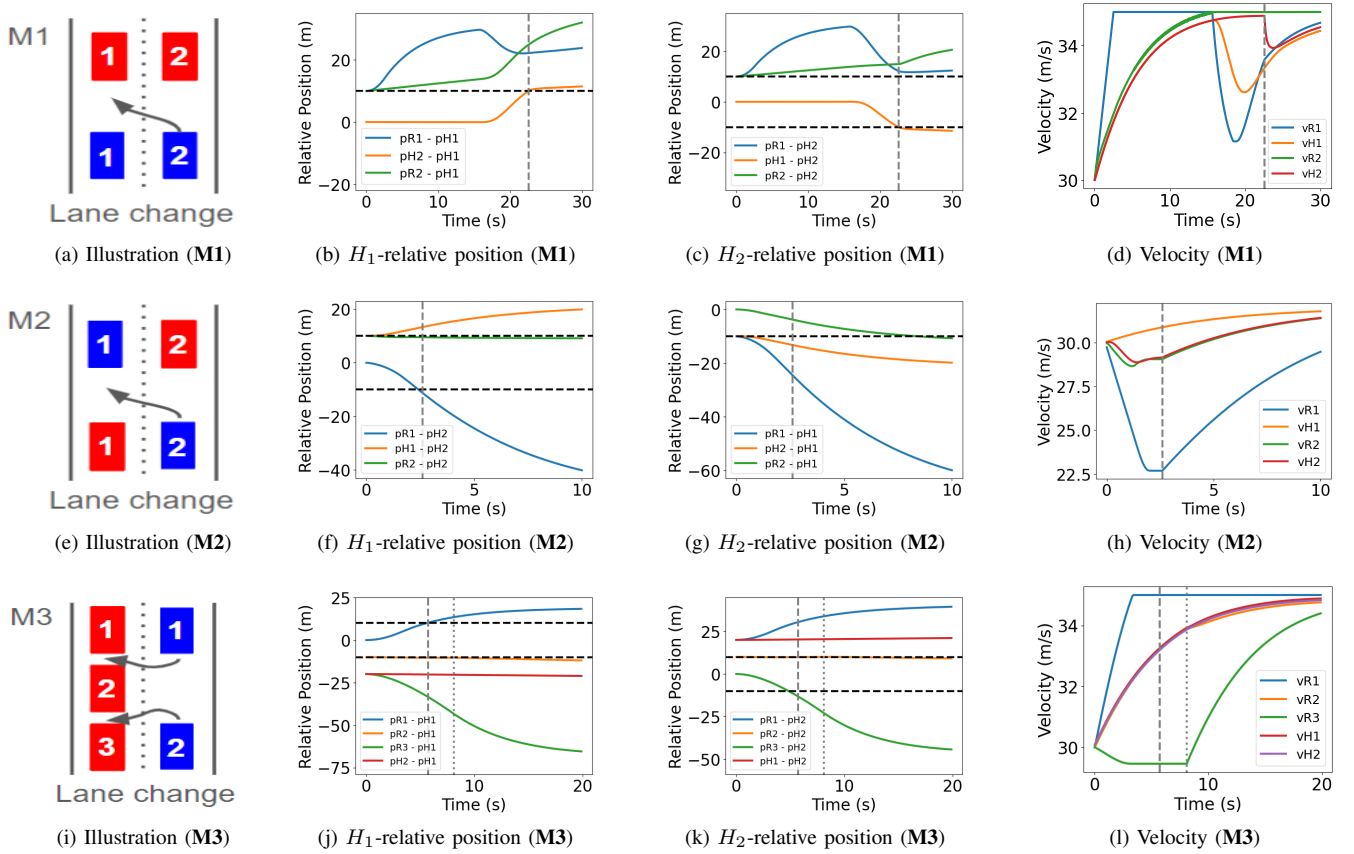


Fig. 3: Illustrations, human-relative position vs. time graphs, and velocity vs. time graphs for scenarios **M1-M3**. In illustrations, red boxes are robot cars, and blue boxes are human-driven cars. In graphs, black dotted horizontal lines denote lower or upper bounds on the value via the influence objective, and gray dotted vertical lines denote the time at which a lane change occurs.

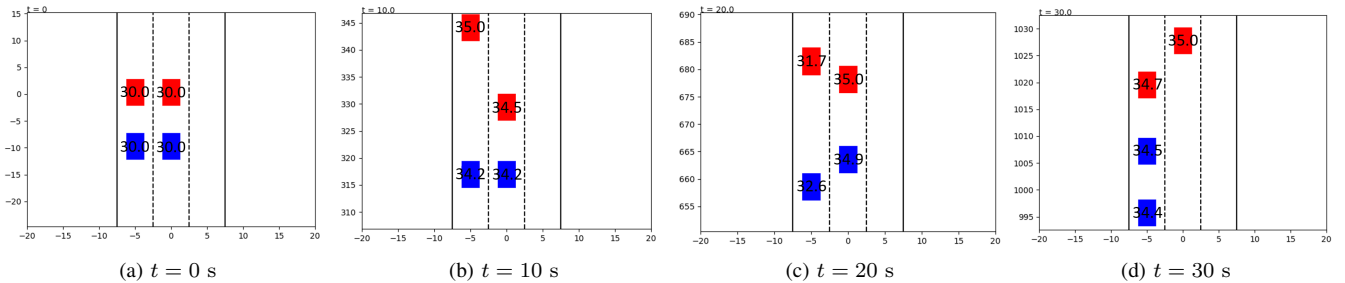


Fig. 4: Visualization of scenario **M1**, where two adjacent lanes each contain a robot car followed by a human-driven car, and the objective is to influence the human in the right lane to merge in between the two cars in the left lane. Red boxes are robot cars and blue boxes are human-driven cars. Overlaying each box is the car’s velocity.

V. CASE STUDIES

In this section, we quantify the effectiveness of our framework and demonstrate its real-world applicability to two high-level objectives.

A. Traffic Flow Optimization

Here we consider a three-lane highway setting where each lane initially contains between 1 and 3 robot cars and between 1 and 3 human-driven cars. The objective of the robot cars is to produce an increase in traffic flow by strategically influencing human-driven car lane changes. In particular, we use one-dimensional k -means clustering on the humans’ desired velocities to assign each car to a lane, where $k = 3$ and each resulting cluster represents a group of cars that should travel in the same lane. The rationale for this lane assignment strategy is that the total traffic flow across a group of lanes is improved when the cars in each lane have similar desired velocities. Once all human-driven cars have been assigned new lanes, each car is influenced to change lanes from its current lane to its assigned lane by the surrounding robot cars (up to 3) using our optimal control framework. Human-driven cars are selected individually for influence by order of index. After all lane changes, each robot car follows IDM control with a desired velocity that matches the highest desired velocity of any human-driven car in its lane.

There is an equal likelihood of each number of robot cars and human-driven cars in each lane, and a given car has an equal likelihood of being a robot car and a human-driven car. For each human-driven car H_i , we generate a desired velocity $v_{H_i} \sim \mathcal{U}(25, 40)$ and a lane-change velocity threshold $\Delta v_i^{th} \sim \mathcal{U}(2, 5)$. We introduce a noise $\mathcal{N}(0, 0.2)$ to each human’s desired following distance, $\mathcal{N}(0, 2)$ to the desired velocity, and $\mathcal{N}(0, 0.1)$ to the desired acceleration, deceleration, and time headway. Each human’s desired lane-change space threshold is equal to the desired following distance. We introduce a noise $\mathcal{N}(0, 0.2)$ to the controls of the human-driven cars.

We use all cars’ average velocity and the average difference between the humans’ desired and actual velocities as metrics for traffic flow, where an increase in the former and a decrease in the latter indicate an improvement in traffic

flow. We simulated 100 trials of this scenario under these conditions, and compared the traffic flow performance prior to and following the human influence maneuvers, at $t = 0$ s and $t = 120$ s, respectively. Fig. 5 shows the average velocity vs. time. Dependent t -tests for paired samples showed a significant increase in average velocity ($t(100) = 3.829, p < 0.001$) and a significant decrease in the difference between desired and actual velocity ($t(100) = 7.146, p < 0.0001$) following the human influence maneuvers. This implies that our framework is effective in improving mixed-autonomy highway traffic flow.

B. Aggressive Behavior Mitigation

Here we consider a single-lane highway setting where a robot car R_1 is preceded by a background car B_1 and followed by a human-driven car H_1 exhibiting aggressive following behavior. This aggressive behavior is encoded as a close following distance, high velocity, and large acceleration and deceleration. The robot car aims to mitigate this behavior by influencing a lower bound s_{min} on the human-driven car’s following distance, an upper bound v_{max} on its velocity, and a lower bound a_{min} and upper bound a_{max} on its acceleration. We formulate each of these intentions as CBF constraints using our framework. We adopt the IDM parameters provided in [26] to define the human’s aggressive following behavior and the desired normal behavior.

We introduce a noise $\mathcal{N}(0, 0.2)$ to the human’s desired following distance, $\mathcal{N}(0, 2)$ to its desired velocity, and $\mathcal{N}(0, 0.1)$ to its desired acceleration, deceleration, and time headway. We also introduce a noise $\mathcal{N}(0, 0.2)$ to the controls of the human and background cars. We fix the initial robot car position $p_{R1} = 0$, and generate an initial human-driven car position $p_{H1} \sim \mathcal{U}(-3\ell, -\ell)$ and background car position $p_{B1} \sim \mathcal{U}(\ell, 3\ell)$. We also generate initial velocities $v_{H1}, v_{R1}, v_{B1} \sim \mathcal{U}(25, 35)$.

We use the average magnitude of jerk as a metric for aggressive following behavior. Higher values of average jerk magnitude were shown in [27] to correlate with higher levels of aggression. We simulated 100 trials of this scenario under these conditions, and compared the average magnitude of jerk from $t = 0$ s to $t = 60$ s with that of a control condition where the robot car instead follows IDM control with normal driving parameters. Fig. 6 shows human

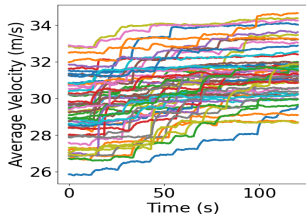


Fig. 5: Average velocity vs. time for traffic flow optimization.

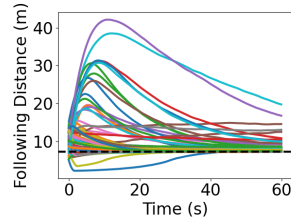


Fig. 6: Human following distance vs. time for aggression mitigation.

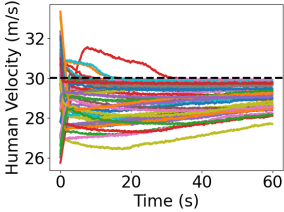


Fig. 7: Human velocity vs. time for aggression mitigation.

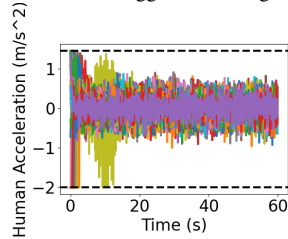


Fig. 8: Human acceleration vs. time for aggression mitigation.

following distance vs. time, Fig. 7 shows human velocity vs. time, and Fig. 8 shows human acceleration vs. time. A dependent t -test for paired samples showed a significant decrease in average jerk magnitude when human influence was employed ($t(100) = 2.368, p < 0.01$). This implies that our framework is effective in mitigating aggressive human following behavior in highway settings.

VI. CONCLUSION

In this work, we presented a novel optimal control framework for influencing human driving behavior in mixed-autonomy traffic. We leveraged control barrier functions to formulate the problem of human influence as a constrained optimization problem on the controls of the surrounding robot cars. We demonstrated our framework's applicability to various objectives and configurations, including multi-robot and multi-human scenarios. We validated its effectiveness in the two real-world objectives of traffic flow optimization and aggressive behavior mitigation. Through our framework, we advance the state of the art by contributing superior versatility in the autonomous influence of human driving behavior. In future work, we intend to expand our framework's compatibility with various human behavior models and further study its flexibility and scalability.

REFERENCES

- [1] E. Yurtsever, J. Lambert, A. Carballo, and K. Takeda, "A survey of autonomous driving: common practices and emerging technologies," *IEEE Access*, vol. 8, pp. 58443–58469, 2020.
- [2] J. Wang, L. Zhang, Y. Huang, J. Zhao, and F. Bella, "Safety of autonomous vehicles," *J. Adv. Transp.*, vol. 2020, pp. 1–13, 2020.
- [3] S. Kaplan, B. Gordon, F. El Zarwi, J. L. Walker, and D. Zilberman, "The future of autonomous vehicles: Lessons from the literature on technology adoption," *Appl. Econ. Perspect. Policy*, vol. 41, no. 4, pp. 583–597, 2019.
- [4] W. Wang, L. Wang, C. Zhang, C. Liu, and L. Sun, "Social interactions for autonomous driving: A review and perspectives," *arXiv [cs.RO]*, 2022.
- [5] R. Pandya, Z. Wang, Y. Nakahira, and C. Liu, "Towards proactive safe human-robot collaborations via data-efficient conditional behavior prediction," *Arxiv.org*. [Online]. Available: <http://arxiv.org/abs/2311.11893>. [Accessed: 15-Mar-2024].

- [6] B. Toghi, R. Valiente, D. Sadigh, R. Pedarsani, and Y. P. Fallah, "Co-operative autonomous vehicles that sympathize with human drivers," in *IEEE/RSJ International Conference on Intelligent Robots and Systems*, 2021.
- [7] D. A. Lazar, R. Pedarsani, K. Chandrasekher, and D. Sadigh, "Maximizing road capacity using cars that influence people," in *IEEE Conference on Decision and Control*, 2018.
- [8] D. Sadigh, S. Sastry, S. A. Seshia, and A. D. Dragan, "Planning for autonomous cars that leverage effects on human actions," in *Robotics: Science and Systems XII*, 2016.
- [9] S. Wang, Y. Lyu, and J. M. Dolan, "Active probing and influencing human behaviors via autonomous agents," *arXiv [cs.RO]*, 2023.
- [10] D. Sadigh, N. Landolfi, S. S. Sastry, S. A. Seshia, and A. D. Dragan, "Planning for cars that coordinate with people: leveraging effects on human actions for planning and active information gathering over human internal state," *Auton. Robots*, vol. 42, no. 7, pp. 1405–1426, 2018.
- [11] W. Xiaorui and Y. Hongxu, "A Lane change model with the consideration of car following behavior," *Procedia Soc. Behav. Sci.*, vol. 96, pp. 2354–2361, 2013.
- [12] L. Sun, W. Zhan, and M. Tomizuka, "Probabilistic prediction of interactive driving behavior via hierarchical inverse reinforcement learning," in *IEEE International Conference on Intelligent Transportation Systems*, 2018.
- [13] T. Li, X. Han, J. Ma, M. Ramos, and C. Lee, "Operational safety of automated and human driving in mixed traffic environments: A perspective of car-following behavior," *Proc. Inst. Mech. Eng. O. J. Risk Reliab.*, vol. 237, no. 2, pp. 355–366, 2023.
- [14] H. Li and S. Zhang, "Lane change behavior with uncertainty and fuzziness for human driving vehicles and its simulation in mixed traffic," *Physica A*, vol. 606, no. 128130, p. 128130, 2022.
- [15] M. Kwon, E. Biyik, A. Talati, K. Bhasin, D. P. Losey, and D. Sadigh, "When humans aren't optimal: Robots that collaborate with risk-aware humans," in *Proceedings of the 2020 ACM/IEEE International Conference on Human-Robot Interaction*, 2020.
- [16] Y. Lyu, W. Luo, and J. M. Dolan, "Adaptive safe merging control for heterogeneous autonomous vehicles using parametric control barrier functions," in *IEEE Intelligent Vehicles Symposium*, 2022.
- [17] K. Xu, W. Xiao, and C. G. Cassandras, "Feasibility guaranteed traffic merging control using control barrier functions," in *American Control Conference*, 2022.
- [18] S. He, J. Zeng, B. Zhang, and K. Sreenath, "Rule-based safety-critical control design using control barrier functions with application to autonomous Lane change," in *American Control Conference*, 2021.
- [19] A. D. Ames, S. Coogan, M. Egerstedt, G. Notomista, K. Sreenath, and P. Tabuada, "Control barrier functions: Theory and applications," in *European Control Conference*, 2019.
- [20] J. F. Fisac, E. Bronstein, E. Stefansson, D. Sadigh, S. S. Sastry, and A. D. Dragan, "Hierarchical game-theoretic planning for autonomous vehicles," in *International Conference on Robotics and Automation (ICRA)*, 2019.
- [21] M. Rowold, A. Langmann, B. Lohmann, and J. Betz, "Open-loop and feedback Nash trajectories for competitive racing with iLQGames," *Arxiv.org*. [Online]. Available: <http://arxiv.org/abs/2402.01918>.
- [22] M. Treiber, A. Hennecke, and D. Helbing, "Congested traffic states in empirical observations and microscopic simulations," *Phys. Rev. E Stat. Phys. Plasmas Fluids Relat. Interdiscip. Topics*, vol. 62, no. 2 Pt A, pp. 1805–1824, 2000.
- [23] J. Grover, N. Mohanty, C. Liu, W. Luo, and K. Sycara, "Noncooperative herding with control barrier functions: Theory and experiments," in *IEEE Conference on Decision and Control*, 2022.
- [24] W. Zhao, T. He, T. Wei, S. Liu, and C. Liu, "Safety index synthesis via sum-of-squares programming," in *American Control Conference*, 2023.
- [25] R. Chen, W. Zhao, and C. Liu, "Safety index synthesis with state-dependent control space," *arXiv preprint*, 2023.
- [26] Y. Li, S. Zhang, Y. Pan, B. Zhou, and Y. Peng, "Exploring the stability and capacity characteristics of mixed traffic flow with autonomous and human-driven vehicles considering aggressive driving," *J. Adv. Transp.*, vol. 2023, pp. 1–21, 2023.
- [27] F. Feng, S. Bao, J. R. Sayer, C. Flannagan, M. Manser, and R. Wunderlich, "Can vehicle longitudinal jerk be used to identify aggressive drivers? An examination using naturalistic driving data," *Accid. Anal. Prev.*, vol. 104, pp. 125–136, 2017.